J Mater Sci: Mater Med (2008) 19:3303–3310
DOI 10.1007/s10856-008-3468-4

SBA-15 ordered mesoporous silica inside a bioactive glass–ceramic scaffold for local drug delivery

V. Cauda · S. Fiorilli · B. Onida · E. Vernè · C. Vitale Brovarone · D. Viterbo · G. Croce · M. Milanesio · E. Garrone

Received: 8 October 2007 / Accepted: 30 April 2008 / Published online: 22 May 2008

Abstract The paper reports the synthesis of an ordered silica mesostructure of the SBA-15 type inside a macroporous bioactive glass–ceramic scaffold of the type SiO_2–CaO–K_2O, to combine the bioactivity of the latter with the release properties of the former, in view of local drug delivery from implants designed for tissue engineering. The standard procedure for SBA-15 synthesis has been modified to minimize the damage to the scaffold caused by the acidic synthesis medium. The composite system has been characterized by means of Scanning Electron Microscopy (coupled with EDS analysis), Small Angle X-Ray Diffraction, Thermogravimetry analysis and Infrared Spectroscopy: the formation of a well ordered hexagonal mesostructure was confirmed. Ibuprofen has been chosen as model drug. The uploading properties have been investigated of the scaffold-mesoporous silica composite as compared with the scaffold as such, and a five-fold increase in the adsorbing properties toward ibuprofen was found, due to the presence of the ordered mesoporous silica. The ibuprofen release to a SBF solution in vitro is complete in 1 day. Retention of bioactivity from the glass–ceramic scaffold after the silica mesostructure incorporation has been observed.

V. Cauda · S. Fiorilli · B. Onida · E. Vernè · C. Vitale Brovarone · E. Garrone (✉)
Dipartimento di Scienza dei Materiali e Ingegneria Chimica, Politecnico di Torino, Torino, Italy
e-mail: edoardo.garrone@polito.it

S. Fiorilli
LaTEMAR, Centre of Excellence funded by MIUR (Italian Ministry for Education, University and Research), Torino, Italy

B. Onida · E. Garrone
INSTM, Unità di Ricerca Torino Politecnico, Torino, Italy

D. Viterbo · G. Croce · M. Milanesio
Dipartimento di Scienze e Tecnologie Avanzate, Università degli Studi del Piemonte Orientale, Alessandria, Italy

1 Introduction

Drug delivery matrices generally consist of organic polymers [1], organic–inorganic hybrid materials and bioactive glasses and ceramics [2–6]. Silica xerogels have been also proposed as carrier for pharmaceutical molecules, directly incorporated into the matrix during polycondensation of inorganic silicate [7]. All these systems exhibit heterogeneous pore size distribution, which leads to a lack of homogeneity in the distribution of guest species throughout the matrix and to a poorly controlled release behavior.

Silica-based ordered mesoporous materials, where all pores show uniform size, arranged in a periodic ordered array, favor the homogeneous distribution of guest molecules, thus representing excellent candidates for controlled release applications. The possibility to modulate the pore diameter in a wide range, by varying the structure-directing agents and synthesis conditions, in principle permits to tailor the kinetics of release through a proper choice of the host matrix pore size with respect to guest molecule dimension. The first study, carried out by Vallet-Regí and coworkers, on the use of the hexagonal mesostructure MCM-41 as ibuprofen delivery system [8], showed the feasibility of employing these matrices, so opening a new investigation area. More recently, several studies concerning the use of mesoporous silicas as drug carriers have appeared, reporting the effect of mesostructure symmetry [9] and pore diameter [10] on the delivery mechanism.

A marked improvement in biomedical applications field could come from combining the release properties shown by the ordered mesoporous systems with the bioactivity of materials employed to fabricate implants. These multifunctional systems would be able not only to promote successful integration of the implanted prosthesis, but also to prevent infections. Moreover, mesoporous materials might even be loaded with osteogenic agents promoting the new bone formation in vivo.

The need of bone regeneration is associated to different diseases, such as bone loss or tumors, periodontal resorption, osteoporosis and arthroplasty revision surgery [11–13]. Among artificial grafts (scaffolds), bioactive glasses of specific composition generally: SiO_2 CaO P_2O_5 MO; M=Na, Mg, etc. have been widely studied in the last years for guided bone regeneration [14–16]. These materials are able to bind to the surrounding bone tissue, through a complex mechanism of ion exchange, silica gel formation and precipitation of a hydroxyapatite layer (HAp) on their surfaces, when in contact with body fluids [17].

Recently, mesoporous materials with chemical composition similar to highly bioactive sol–gel glasses have been reported, with the purpose of their application in the field of bone tissue regeneration [18–20].

The present contribution reports the synthesis of SBA-15-type ordered mesoporous silica particles inside the macroporous structure of a bioactive glass–ceramics scaffold glass belonging to the SiO_2–CaO–K_2O (hereafter SCK) system, in view of combining the release properties shown by the ordered mesoporous systems with the bioactivity and mechanical properties of materials employed for tissue engineering. To our knowledge the only study, showing some similarities with the present paper, concerns the coating of a bioactive glass with mesoporous SBA-15 silica thin film [21], which was found to enhance the bioactivity of the system.

Ibuprofen, extensively adopted in the literature to study the uploading and delivering properties of mesoporous silicas [8–10], has been chosen as model drug to characterize the role of silica mesostructure in the incorporation capacity and the release behavior of the obtained composite system.

A preliminary study on the incorporation of SBA-15 silica inside the same scaffold [22] showed the feasibility of this synthesis approach; here, a detailed structural characterization of the SBA-15-scaffold composite is reported, together with ibuprofen release kinetics and bioactivity essays carried on the composite system.

The proposed procedure might be of more general interest in that it could be used to prepare porous composite systems, with controlled porosity ranking from macropores to mesopores, for different applications, such as adsorption, storage and catalysis.

2 Experimental

2.1 Preparation of SCK scaffold

A glass belonging to the SiO_2–CaO–K_2O system, having the molar composition 50% SiO_2: 44% CaO 6%: K_2O has been used to produce the scaffold. The glass, previously characterized [23], was prepared by melting the raw products in a platinum crucible at 1500°C for 1 h and by quenching the molten glass into water to obtain a frit. This was ground by ball milling and sieved to a grain size below 106 μm; the glass particles were then mixed with 60% vol. of polyethylene particles with size between 300 and 600 μm, uniaxially pressed (150 MPa) for 10 s [24], then treated at 950°C for 2 h in air to induce both the sintering of SCK particles and the removal of the organic phase.

Compressive tests were carried out on 3 cubic samples 1 cm × 1 cm × 1 cm using an Instron machine. The compressive strength was calculated from the maximum load registered during the test divided by the loaded area. Moreover to study the isotropy of the prepared scaffold, the compressive strength was evaluated in the three directions to assess any possible anisotropy [23].

This sample will be referred hereafter to SCK.

2.2 Preparation of SBA-15-SCK composite scaffold

The mesophase solution was prepared following the recipe for SBA-15 synthesis reported in Ref. [25]. A solution of the triblock copolymer P123 [$(EO_{20}PO_{70}EO_{20})$, kindly provided by BASF] was prepared in acidic (HCl, Fluka) media (pH < 1), followed by the addition of tetraethylorthosilicate (TEOS, Aldrich). The reactant molar ratio was: P123 0.017: TEOS 1: HCl 6: H_2O 167.

The procedure to precipitate the mesostructure within the SCK consists in two steps, i.e. *hydrolysis* of TEOS in SBA-15-synthesis solution and *dipping* of a SCK disk into the synthesis batch. *Hydrolysis* and *dipping* times have been chosen to ensure, on the one hand, the assembly of an ordered mesostructure within the scaffold and, on the other hand, to prevent scaffold damage due to the acidity of the synthesis solution.

Soaking for a period longer than 15 min led to a damage of the scaffold.

Literature results from ^{1}H NMR, TEM [26] and SAXS-XRD [27] measurements carried out in the early stage of assembly of SBA-15 alone indicate that 25–30 min of reaction time, after the addition of silica precursor, are necessary for the formation of silica-surfactant hybrid micelles, which later assembly in the hexagonal packing.

Therefore, *hydrolysis* and *dipping* times were chosen to guarantee a sufficient reaction after TEOS addition, not exceeding, however, 30 min.

Fifteen minutes of *hydrolysis*, followed by soaking a scaffold disk for 15 min (*dipping*) were found to be the best compromise: shorter *hydrolysis* time before scaffold soaking led to a poorly ordered mesostructure within SCK macropores.

After soaking, the SCK disk was separated from the solution batch and aged in a closed vessel for 72 h at 60°C. The ageing phase promotes the complete condensation of silica network, favoring the formation of the ordered mesostructure [28]. Remove of the template was carried out by heating the sample in air up to 350°C (1°C/min) and then heating at the same temperature for 4 h. This sample will be referred hereafter to SBA-15-SCK.

To evaluate how the scaffold surface, and in turn its adsorbing properties, are affected by the contact with the acidic solution during the mesostructure incorporation, a sample of SCK was soaked for 15 min in a solution having the same composition as the synthesis solution but without TEOS (this sample is referred to SCK-treated).

2.3 Characterization

Small angle X-ray diffraction experiments were carried out by the Austrian SAXS beam line (BL 5.2 L) [29] of the ELETTRA Synchrotron Light Laboratory (Trieste, Italy), using X-rays of wavelength $\lambda = 0.077$ nm and the data were collected with a 2D CCD-detector (diameter 115 mm; Photonic Science, Robertsbridge, UK), positioned at 1773.7(9) mm from the sample. The two-dimensional data were corrected and processed using the FIT2D program [30, 31]. The reconstruction of the electron density distribution (2D electron density maps), from a limited number of reflections, was carried out using the model described elsewhere [27, 32], from which structural parameters, such as pore diameters and wall thicknesses, may be evaluated.

Field Emission Scanning Electron Microscopy (Assing FESEM Supra 25) associated with Energy Dispersive Spectroscopy (EDS, Oxford Instrument INCA X-Sight), thermogravimetry (Mettler Toledo, TGA/SDTA) were also used to characterize the samples. Infrared spectra were recorded on a Bruker Tensor 37 equipped with a 670 HYPERION infrared microscope, operating in attenuated reflection mode (ATR).

2.4 Drug up-take and release

Adsorption of ibuprofen (99.9%, Sigma) has been carried out putting in contact for 3 days at room temperature a solution of ibuprofen in pentane (33 mg/ml) with respectively the SBA-15-SCK, SCK and SCK-treated.

After the immersion, the UV–Vis spectrum of the solution was measured and the amount of ibuprofen absorbed by the different systems, through a calibration curve based on the typical absorption band at 263 nm. Drug delivery in vitro has been evaluated by soaking the samples in a stirred simulated body fluid (SBF) [33] maintained at 37°C and collecting the spectrum of the solution at different times.

All UV–visible spectra were recorded with a Cary 500 Scan UV–visible spectrophotometer. The assessment of in vitro bioactivity was carried out on SBA-15-SCK composite scaffold, by soaking the composite system in SBF at 37°C for 1 month and following the formation of HAp layer by means of SEM.

The pH of solution was monitored by microprocessor pH meter (HANNA Instruments pH 211).

3 Results and discussion

3.1 Morphology and characterization

The morphology of the SCK is reported in Fig. 1; the scaffold is characterized by interconnected pores in the range 100–600 μm and pores of 1–10 μm [23]. The total pore volume is around 62 ± 1%: the scaffold compressive strength is about 1.5 ± 0.5 MPa, as required for a material to be used as bone substitute [23].

Field Emission SEM pictures of SBA-15-SCK (Fig. 2) reveal the presence of silica grains sitting in the macropores of the scaffold, with dimension between 500 nm and few microns, with well-defined morphology, reflecting the hexagonal symmetry of SBA-15. EDS analysis carried out on these grains indicated the presence of oxygen and silicon in an atomic percentage ratio very close to the theoretical value of 2, confirming a SiO_2-based composition.

It is interesting to note that, though the followed synthesis procedure to precipitate SBA-15 inside the scaffold is that reported by Zhao et al., mesostructured silica did not adopt the rod-like domains morphology aggregated into fiber-like macrostructures, typical of SBA-15 materials, but were characterized by polyhedral crystals. This morphology has been observed when nonionic block-copolymer-templated silica are prepared in the presence of inorganic salts [34, 35]. The effect of inorganic salts on the morphology of mesoporous materials have been explained by Yu et al. in terms of *colloidal phase separation mechanism* (CPSM), which interprets the final morphology of mesoporous materials as the result of the competition between the free energy formation of mesostructure self-assembly (ΔG) and the surface free-energy (F) of the liquid-crystal phase. When the colloidal phase separation occurs early ΔG is dominant in the synthesis system and the morphology of the particles is developed together with the formation of the mesophase; on the other hand if the phase

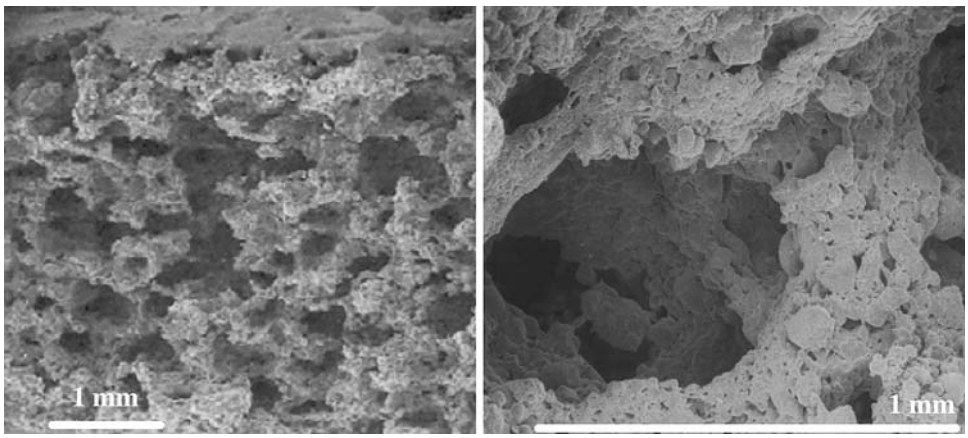

Fig. 1 SEM micrographs of the as-prepared SCK scaffold

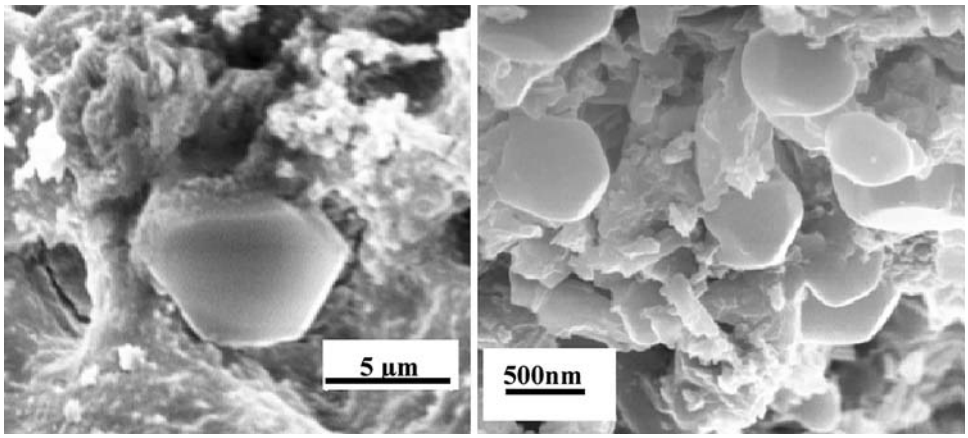

Fig. 2 SEM micrographs of SBA-15-SCK composite scaffold after calcination

separation occurs more slowly F will play a more important role in determining the final morphology, being the latter basically influenced by surface energy effects: a large curvature morphology (e.g. spherical) will be generated. Inorganic salts play an important role in the synthesis of mesoporous single crystal [36, 37], and colloidal phase separation mechanism may be used to interpret this effect on mesoporous materials morphology. Indeed, high ionic strength favors the aggregation of surfactant/silica aggregates, whose approach to each other is unfavorable due to the electrostatic repulsion, and thus favoring the phase separation process [35]. From CPSM, a quick phase separation process leads to the formation of mesostructures where ΔG is dominant with respect to surface energy effect (F): therefore, in the presence of inorganic salts mesoporous materials with crystal-like morphologies can be generated [35]. The presence of crystal-like morphology for SBA-15 mesostructure within the scaffold macropores may be due to the local ions concentration inside the SCK porosity, caused by a partial solubilization of the scaffold in acidic medium, with release of K^+, Ca^{2+} and silicate ions in solution.

SEM pictures also indicate that the SCK was not inert to the strong acidic conditions used to precipitate SBA-15: a partial degradation of the pore morphology of the scaffold was observed, due the dissolution of the of the glass–ceramic system.

Figure 3 shows the synchrotron radiation diffraction patterns of the as-synthesized and the surfactant-free SBA-15-SCK samples. The patterns indicate the presence of three weak peaks for the as-synthesized sample and of six peaks for the calcined sample. In the latter, a substantial increase in the intensity of (100), (110) and (200) peaks is also observed, due to the removal of the surfactant [38]. Reflection peaks are consistent with the presence of an ordered 2D hexagonal SBA-15 type mesostructure. The cell parameter decreases from 12.8 nm for the as-synthesized sample to 12.4 nm for the calcined one.

The integrated intensities of the surfactant-free SBA-15-SCK peaks were also used for the calculation of the 2D electron density maps. The multiplicity for this hexagonal phase was established using the approach described by Impéror-Clerc et al. [39] and the phase problem was solved by sign permutation, according to the procedure described by Flodström et al. [27]. The sign sequence $- - + + + +$ was found to be more realistic and sensible with respect to the a-priori information [27]. The reconstruction of the electron density distribution (Fig. 4) allows to estimate the

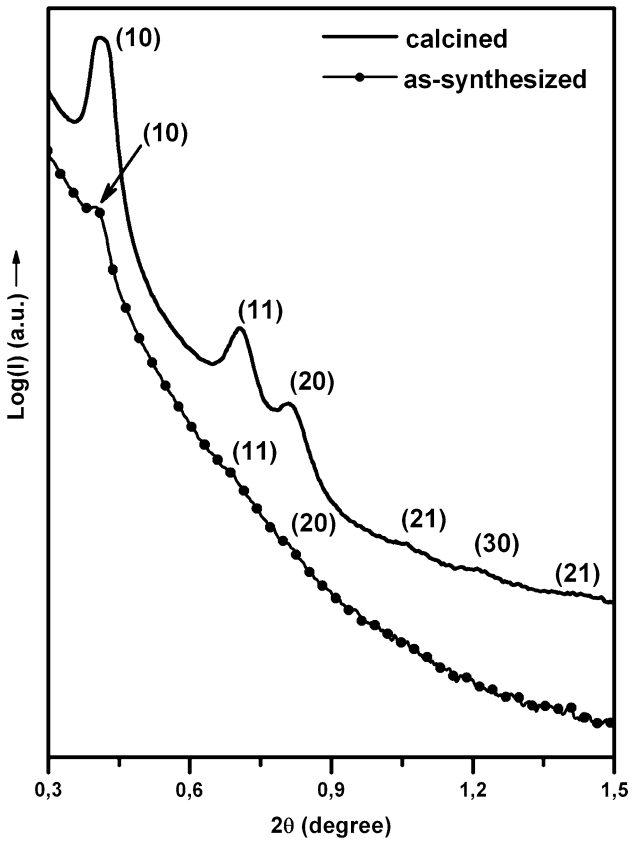

Fig. 3 X-ray diffraction patterns of as-synthesized and calcined SBA-15-SCK

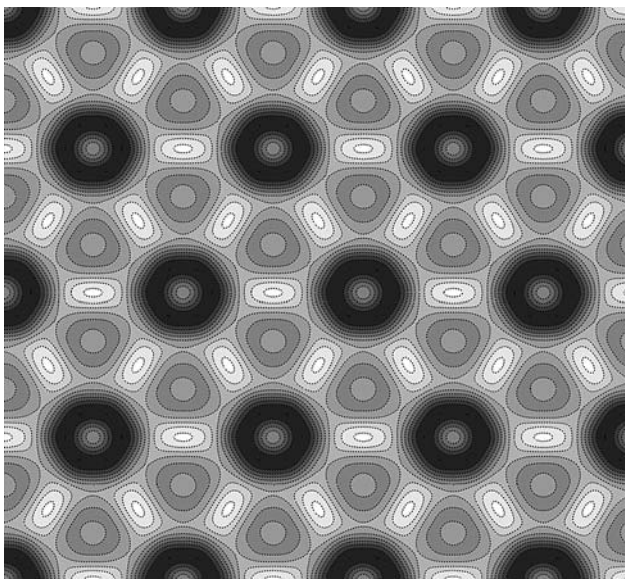

Fig. 4 Calculated 2D electron density map of the calcined SBA-15-SCK composite. Grey areas correspond to regions of high electron density and dark areas to regions of low electron density

average dimension of the pores of the SBA phase (7.7 nm) and the average wall thickness (3.7 nm) in the calcined sample. These are in very good agreement with the experimental values obtained by N_2 adsorption/desorption isotherm [22].

It is worth of note that, although synthesis conditions are rather different from the standard procedure for SBA-15 silica preparation, also due to the influence of inorganic salts coming from the partial scaffold dissolution, as commented above, pore size and wall thickness shown by silica phase within the scaffold are very similar to those reported for SBA-15 materials [25].

Thermogravimetric analysis carried out on as-synthesized sample revealed that the weight loss, due to decomposition of the organic template, occurs in the 150–350°C range. Thermogravimetry, coupled to mass spectrometry, carried out on sample calcined at 350°C, did not reveal any presence of residual organic species.

Thermogravimetric data allow an evaluation of the amount of mesoporous silica inside composite system, by comparing the amount of organic template, due to silica mesostructure in the composites, with the quantity of surfactant of SBA-15 in powder form: the estimated amount of silica mesostructure was found to be around 12% in weight.

3.2 Ibuprofen upload and release

Ibuprofen uploading properties of scaffold-mesostructure composite have been investigated and compared to the behavior of SCK and SCK-treated.

The weight percentage of ibuprofen reached a value of about 2% for SCK, 3% for SCK-treated and 11.5%, i.e. about five times higher, for SBA-15-SCK, evidencing the role of mesoporous silica in the drug uptake (Scheme 1). After soaking in acid solution, SCK adsorbs more drug: this suggests that the surface is affected somewhat by the treatment.

Figure 5 reports FTIR spectra of SBA-15-SCK before and after drug uptake. Before drug uptake, the system shows in the high frequency region a weak broad band centered at 3400 cm^{-1} due to H-bonded hydroxyls. No

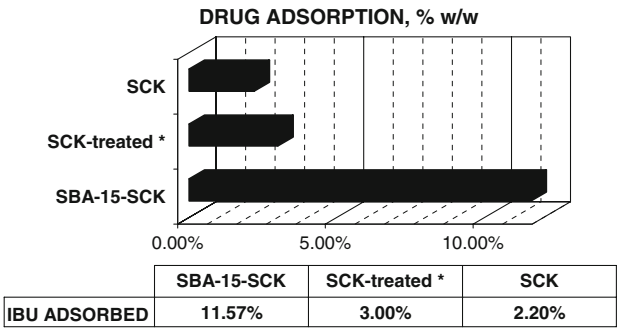

	SBA-15-SCK	SCK-treated *	SCK
IBU ADSORBED	11.57%	3.00%	2.20%

Scheme 1 Load of ibuprofen SBA-15-SCK composite scaffold compared with SCK-treated and SCK as such. * Same reagents composition of synthesis solution without TEOS

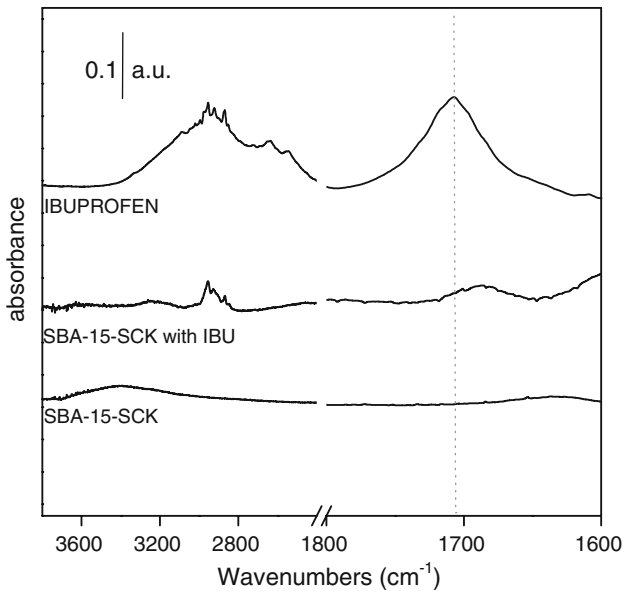

Fig. 5 FTIR spectra of SBA-15-SCK composite scaffold before and after ibuprofen adsorption (SBA-15-SCK with IBU) and of the drug alone (IBU). Spectra show a break in 2,400–1,800 cm^{-1} range

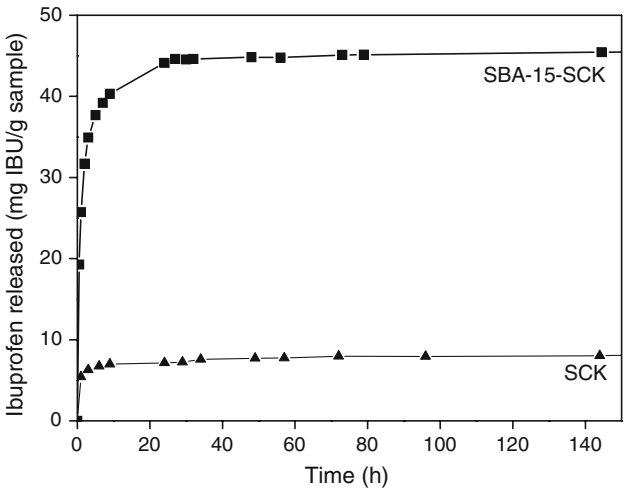

Fig. 6 Release curves in SBF at 37°C of ibuprofen entrapped in SBA-15-SCK and in SCK

signals due to the aliphatic C–H stretching are visible below 3000 cm^{-1}, so confirming the complete removal of template. After drug adsorption, typical bands of ibuprofen molecule are visible, i.e. the aromatic (above 3000 cm^{-1}) and aliphatic (below 3000 cm^{-1}) C–H stretching mode. The low-frequency region shows the C=O stretching band at 1685 cm^{-1}, at slightly lower values than that found for ibuprofen in the solid state (1705 cm^{-1}), most probably because of the formation of a hydrogen bond between the carboxylic group of ibuprofen molecule and a hydroxyl group on silica surface.

The delivery profiles of ibuprofen from SBA-15-SCK composite scaffold and from SCK as function of time are reported in Fig. 6. On the one hand, the composite system released a larger amount of drug compared to the scaffold alone, as expected on the basis of the adsorption capacity of the two systems. On the other hand, the release from the two systems occurred with very similar kinetics, indicating that the mesoporous silica acted as reservoir of the drug molecules, without altering sizably the release rate of the model drug. In particular, the composite system shows a fast increase of drug concentration in SBF between 0 and 8 h; after this burst effect, a slower release is observed between 8 and 24 h. After, a plateau is observed. Similar release profile of ibuprofen from calcined SBA-15 in powder form have been reported by Song et al. [40], who observed a complete release of the drug in 10 h. Instead for SBA-15-SCK composite, approximately 40% w/w of the incorporated drug is released. We suggest that the reason of a partial release from the composite system is a pore occlusion occurring during the contact time between the composite scaffolds and the SBF solution. In fact the bioactivity of the system, i.e. SCK, may induce precipitation of apatite precursors on the mesostructure in the very first hours of soaking in SBF solution. These precipitated species might partially block mesopores, preventing further drug diffusion out of the silica matrix. Furthermore, the capacity to promote apatite-like layers has been also reported for SBA-15 mesostructured silica [10].

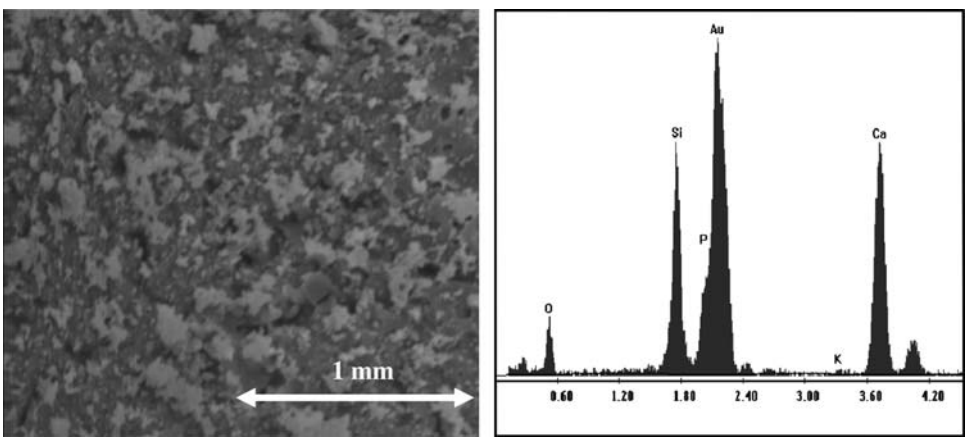

Fig. 7 SEM micrograph and EDS analysis of SBA-15-SCK after 1 month in SBF at 37°C

Bioactivity essays have been carried out on SBA-15-SCK, to check whether the incorporation of mesoporous silica does reduce bioactivity of the scaffold. Figure 7 shows a SEM picture of the sample after 1 month in SBF at 37°C: globular HAp nuclei are present on the surface. EDS analysis confirms the presence of calcium and phosphorus on the surface, their ratio being close to 10:6, required by the HAp chemical formula. This suggests that contact with the acidic synthesis solution and the presence of silica grains have not altered the overall bioactivity of the scaffold.

4 Conclusions

The procedure to synthesize SBA-15-type mesoporous silica properly adapted for the incorporation in the macropores of a bioactive glass–ceramic SCK scaffold, has led to a scaffold-mesophase composite system. This shows ibuprofen up-take capacity about five times higher than the scaffold alone, showing that this approach is efficient in increasing drug up-loading.

Ibuprofen release from SBA-15-scaffold composite occurs with a fast kinetics and is complete in 1 day, suggesting a negligible host-guest effect of SBA-15 pores on drug retention. Loading and release experiments on SBA-15-SCK composite scaffold with bulkier molecules are in progress to investigate the role of the host matrix in determining the delivery kinetics of guest species.

Besides, in order to modulate the delivery rate, the incorporation inside the same SCK scaffold of MCM-41-type spheres, with narrower pore size with respect to SBA-15, has been carried out and presented in a separated paper by the authors [41]. Furthermore, it was interesting to explore the effect of basic conditions, required to precipitate MCM-41 synthesis, instead of those, strongly acidic, used for the preparation of SBA-15, on the bioactivity and mechanical properties of the final composite system.

Bioactivity assay carried out on SCK-SBA-15 composite has revealed that the presence of silica grains does not alter sizably the overall bioactivity of the scaffold.

In conclusion, this study shows the feasibility of combining the properties of glass–ceramic scaffolds with ordered mesoporous silica as drug carrier in view of local drug release.

Acknowledgments Financial support of MIUR, Italy (project PRIN 2004) is acknowledged.

References

1. A. Rösler, G.W.M. Vandermuelen, H.A. Klok, Adv. Drug Deliv. Rev. **53**, 95 (2001)
2. S. Padilla, R.P. Del Real, M. Vallet-Regí, J. Control. Release **83**, 34 (2002)
3. A. Rámila, R.P. Del Real, R. Marcos, P. Horcajada, M. Vallet-Regí, J. Sol–Gel Sci. Technol. **26**, 1195 (2003)
4. K.-D. Kvhn, in *Bone Cements* (Springer, Berlin, 2000)
5. D. Arcos, C.V. Ragel, M. Vallet-Regí, Biomaterials **22**, 701 (2001)
6. S.R. Hall, D. Walsh, D. Green, R. Oreffob, S. Mann, J. Mater. Chem. **13**, 186 (2003)
7. M. Ahola, P. Kortesuo, I. Kangasniemi, J. Kiesvaara, A. Yli-Urpo, Int. J. Pharmcol. **195**, 219 (2000)
8. M. Vallet-Regí, A. Rámila, R.P. Del Real, J. Pérez-Pariente, Chem. Mater. **13**, 308 (2001)
9. I. Izquierdo-Barba, A. Martinez, A.L. Doadrio, J. Pérez-Pariente, M. Vallet-Regí, Eur. J. Pharm. Sci. **26**, 365 (2005)
10. P. Horcajada, A. Rámila, J. Pérez-Pariente, M. Vallet-Regí, Microporous Mesoporous Mater. **68**, 105 (2004)
11. P. Sepulveda, J.R. Jones, L.L. Hench, J. Biomed. Mater. Res. **59**, 340 (2002)
12. Y. Lee, Y. Seol, Y. Lim, S. Kim, S. Han, I. Rhyu, S. Baek, S. Heo, J. Choi, P. Klokkevold, C. Chung, J. Biomed. Mater. Res. **54**, 216 (2001)
13. P. Sepulveda, A.H. Bressiani, J.C. Bressiani, L. Meseguer, B. Konig, J. Biomed. Mater. Res. **62**, 587 (2002)
14. L.L. Hench, Curr. Opin. Solid State Mater. Sci. **2**, 604 (1997)
15. Z. Cong, W. Jianxin, F. Huaizhi, L. Bing, Z. Xingdong, J. Biomed. Mater. Res. **55**, 28 (2001)
16. H. Ramay, M. Zhang, Biomaterials **24**, 3293 (2003)
17. L.L. Hench, J. Am. Ceram. Soc. **74**, 1487 (1991)
18. X. Yan, C. Yu, X. Zhou, J. Tang, D. Zhao, Angew. Chem. Int. Ed. **43**, 5980 (2004)
19. A. López-Noriega, D. Arcos, I. Izquierdo-Barba, Y. Sakamoto, O. Terasaki, M. Vallet-Regí, Chem. Mater. **18**, 3137 (2006)
20. Q. Shi, J. Wang, J. Zhang, J. Fan, G.D. Stucky, Adv. Mater. **18**, 1038 (2006)
21. J.M. Gomez-Vega, A. Hozumi, E. Saiz, A.P. Tomsia, H. Sugimura, O. Takai, J. Biomed. Mater. Res. **56**, 382 (2001)
22. B. Onida, V. Cauda, S. Fiorilli, E. Vernè, C. Vitale, D. Viterbo, G. Croce, M. Milanesio, E. Garrone, Stud. Surf. Sci. Catal. **158b**, 2027 (2005)
23. C. Vitale Brovarone, S. Di Nunzio, O. Bretcanu, E. Verné, J. Mater. Sci. Mater. Med. **15**, 209 (2004)
24. C. Vitale Brovarone, E. Verné, M. Borsetti, P. Appendino, M. Cannas, J. Mater. Sci. Mater. Med. **16**, 909 (2005)
25. D. Zhao, J. Feng, Q. Huo, N. Melosh, G.H. Fredrickson, B.F. Chmelka, G.D. Stucky, Science **279**, 548 (1998)
26. K. Flodström, H. Wennerström, V. Alfredsson, Langmuir **20**, 680 (2004)
27. K. Flodström, C.V. Teixeira, H. Amenitsch, V. Alfredsson, M. Lindén, Langmuir **20**, 4885 (2004)
28. H. Yang, Q. Shi, B. Tian, S. Xie, F. Zhang, Y. Yan, B. Tu, D. Zhao, Chem. Mater. **15**, 536 (2003)
29. H. Amenitsch, M. Rappolt, M. Kriechbaum, H. Mio, P. Laggner, S. Bernstorff, J. Synchrotron Radiat. **5**, 506 (1998)
30. A.P. Hammersley, in *FIT2D V5.18 Reference Manual V1.6.*, ESRF Internal Report, EXP/AH/95-01 1995
31. A.P. Hammersley, S.O. Svensson, M. Hanfland, A.N. Fitch, D. Häusermann, High Press. Res. **14**, 235 (1996)
32. P.E. Harper, D.A. Mannock, R.N.A.H. Lewis, R.N. Mcelhaney, S.M. Gruner, Biophys. J. **81**, 2693 (2001)
33. T. Kokubo, H. Kushitani, S. Sakka, T. Kisugi, T. Yamamuro, J. Biomed. Mater. Res. **24**, 721 (1990)
34. C. Yu, B. Tian, J. Fan, G.D. Stucky, D. Zhao, J. Am. Chem. Soc. **124**, 4556 (2002)
35. C. Yu, J. Fan, B. Tian, D. Zhao, Chem. Mater. **16**, 889 (2004)
36. R. Ryoo, S. Jun, J. Phys. Chem. B **101**, 317 (1997)
37. W. Zhang, B. Glomski, T.R. Pauly, T.J. Pinnavaia, Chem. Commun. 1803 (1999)

38. F. Kleitz, W. Schmidt, F. Schüth, Microporous Mesoporous Mater. **65**, 1 (2003)
39. M. Impéror-Clerc, P. Davidson, A. Davidson, J. Am. Chem. Soc. **122**, 11925 (2000)
40. S.W. Song, K. Hidajat, S. Kawi, Langmuir **21**, 9568 (2005)
41. R. Mortera, B. Onida, S. Fiorilli, V. Cauda, C. Vitale, F. Baino, E. Vernè, E. Garrone, Chem. Eng. J. **137**, 54 (2008)